

J. Verrelst*, J.P. Rivera, G Camps- Valls & J. Moreno
Image Processing Laboratory (IPL), University of Valencia, Spain

1. Introduction

New retrieval algorithms for Sentinel-2

The Copernicus Sentinel-2 (S2) satellite missions are designed to provide globally-available information on an operational basis for services and applications related to land. S2 is configured with improved spectral capabilities. Also **improved and robust algorithms for biophysical parameter retrieval are demanded**. This work present an overview of state-of-the-art retrieval methods dedicated to the quantification of terrestrial biophysical parameters. The rationale of all these methods is that spectral observations are in a way related to the parameters of interest. In all generality, retrieval methods can be categorized into three families: (i) **parametric regression**, (ii) **non-parametric regression**, and (iii) **Inversion methods**.

We have recently developed retrieval modules within the **ARTMO toolbox** that provide a suite of methods of these three families. As such, consolidated findings can be achieved about which type of retrieval method is most accurate, robust and fast.

Objective:

To evaluate systematically 3 families of biophysical parameter retrieval methods for improved LAI estimation by using a local dataset (SPARC) and simulated S2 observations.

2. Data & Experimental setup

Ground truth data:

- SPARC dataset (Barrax, Spain): **103 LAI points** over various crop types and phenological stages.

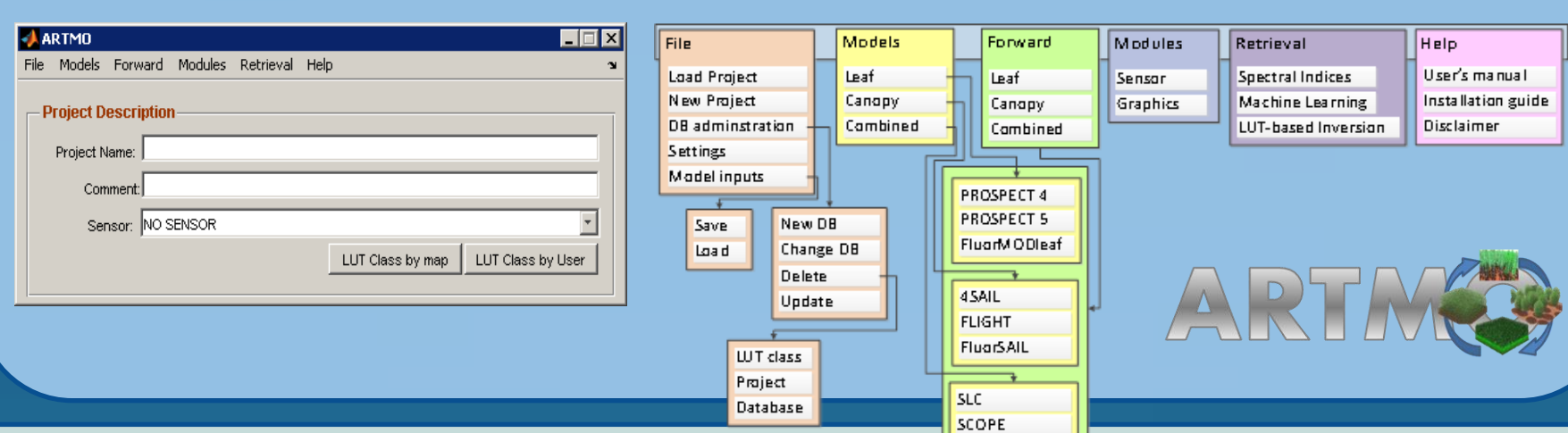
Simulated Sentinel-2 observations:

- **HyMap** flight line acquired during SPARC.
- **Resampled to Sentinel-2 settings.**

| Band # | B1 | B2 | B3 | B4 | B5 | B6 | B7 | B8 | B8a | B9 | B10 | B11 | B12 |
|------------------------|-----|-----|-----|-----|-----|-----|-----|-----|-----|-----|------|------|------|
| Band center (nm) | 443 | 490 | 560 | 665 | 705 | 740 | 783 | 842 | 865 | 945 | 1375 | 1610 | 2190 |
| Band width (nm) | 20 | 65 | 35 | 30 | 15 | 15 | 20 | 115 | 20 | 20 | 30 | 90 | 180 |
| Spatial resolution (m) | 60 | 10 | 10 | 10 | 20 | 20 | 20 | 10 | 20 | 60 | 60 | 20 | 20 |

Experimental setup:

- Only S2 bands of 10 m (coarse-grained to 20 m) and 20 m were used (**10 bands**).
- 50% of data (ground truth & associated S2 spectra) for training (Spectral Indices, MLRA) and **50% for validation (same for all retrieval approaches)**.
- Comparison through goodness-of-fit measures: R², RMSE, NRMSE



6. Conclusions

With view of biophysical parameters retrieval (e.g. LAI) from Sentinel-2 (20 m), three families of biophysical parameter retrieval methods have been systematically analyzed against the same validation dataset (SPARC, Barrax, Spain). Users typically require an accuracy with relative errors below 10%. It led to the following conclusions:

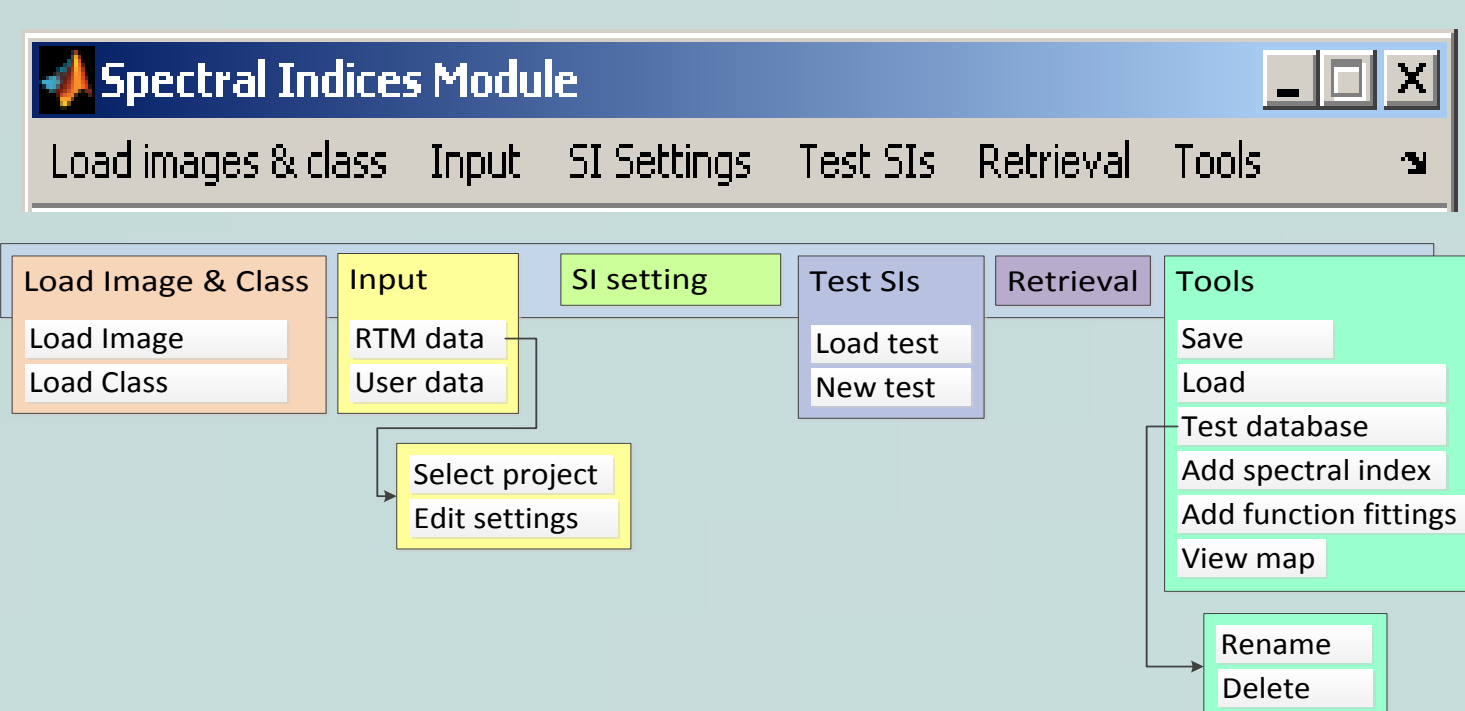
Parametric - Spectral Indices: All 2-, 3- and 4-band combinations according to normalized difference (ND) have been analyzed. A 4-band index with bands in SWIR was best performing, but the 10% error was not reached (NRMSE: 16.0%; R²: 0.79). Most critically, the absence of uncertainty estimates makes this method cannot be considered as reliable. Fast mapping (1s.).

Nonparametric - MLRAs: These are powerful and also fast regressors. Several yielded high accuracies with errors below 10% (KRR, GPR, VHGPR, ELR)! Particularly GPR (NRMSE: 8.2; R²: 0.91) is of interest as it delivers insight in relevant bands and associated uncertainties. Hence, unreliable retrievals (e.g. <20%) can be masked out. Fast mapping (7s.).

LUT-based Inversion: A PROSAIL LUT of 100000 simulations has been prepared and various cost functions and regularization options were applied. Best cost functions performed on the same order as best 2-band SIs (16.6%; R²: 0.76). Because inverted against a LUT table pixel-by-pixel, biophysical parameter mapping went unacceptably slow (> 25h.).

3. (i) Parametric regression: Spectral Indices - LAI

ARTMO's Spectral Indices (SI) module:



In the **Spectral Indices** module the predictive power of all possible 2-, 3- or 4-band combinations according to an Index formulation (e.g. simple ratio (SR), normalized difference (ND)) to a biophysical parameter can be evaluated.

Applied SI formulations:

- 2-band SIs:
 - **SR (B2/B1)** (10² combinations)
 - **ND (B2-B1)/(B2+B1)** (10² combinations)
- ND 3-band **(B2-B1)/(B2+B3)** (10³ combinations)
- ND 4-band **(B2-B1)/(B3+B4)** (10⁴ combinations)

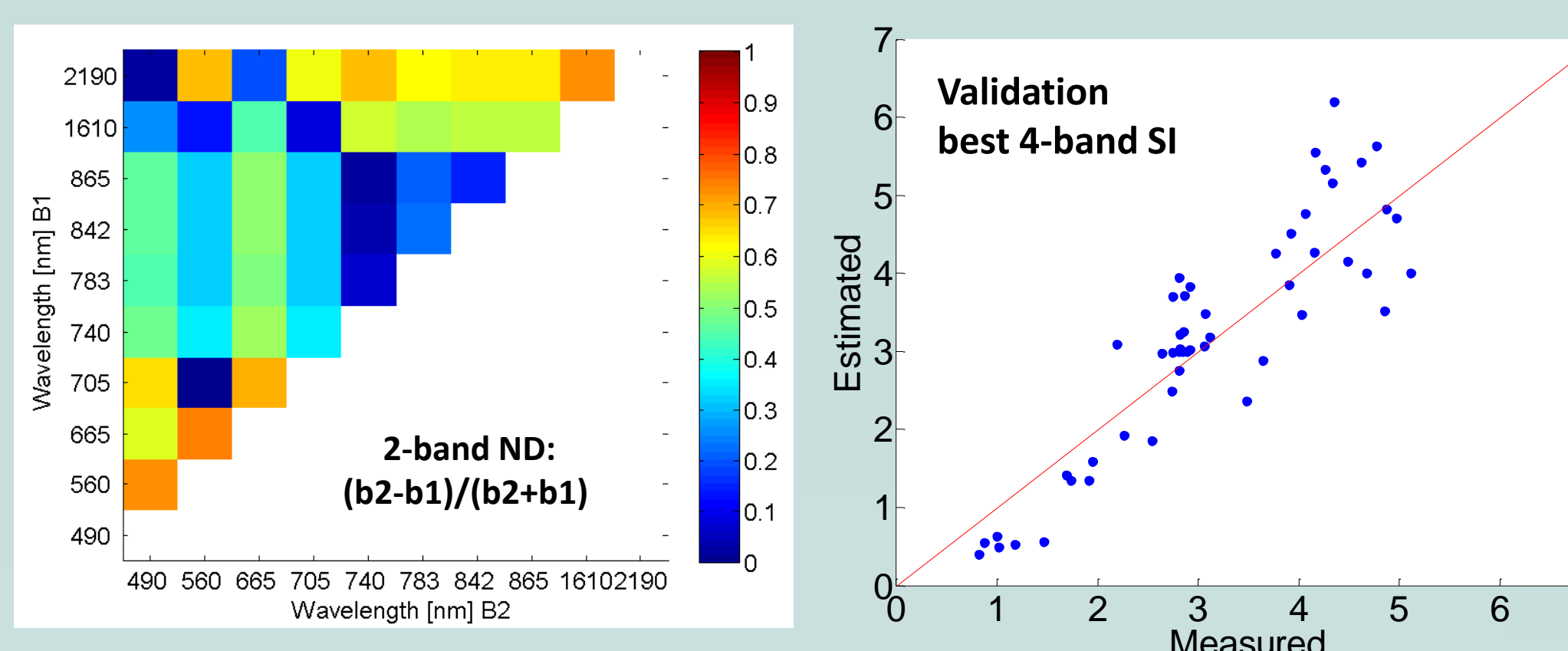
A Linear regression was applied.

Very fast: **0.004 sec** per SI model (11200 SI models in 42.8 s.)

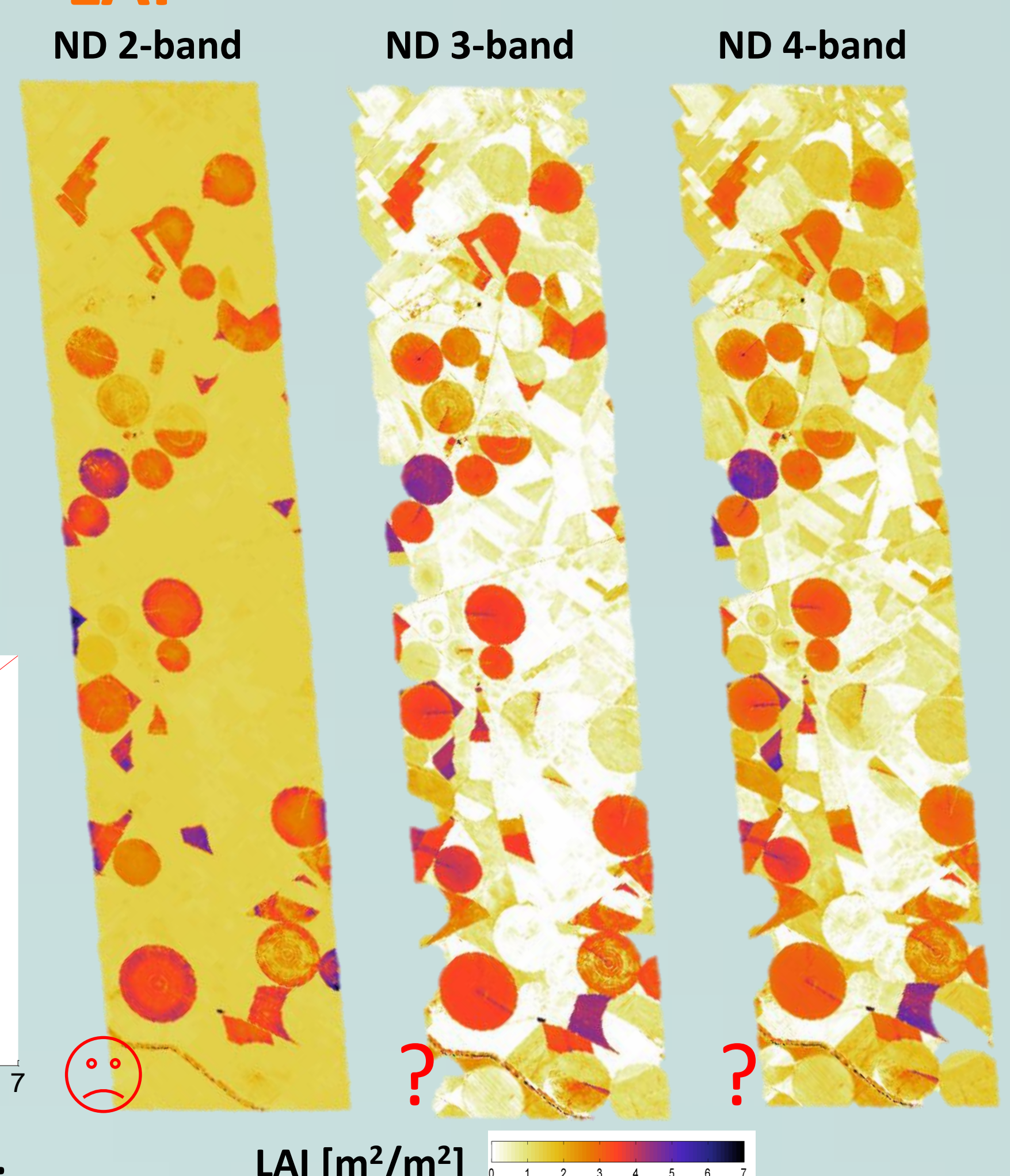
Best validated SIs (**50% validation data**) ranked according to R²:

| SI formulation | Best band combination (B1, B2, B3, B4) | RMSE | NRMSE | R ² |
|------------------------------------|--|------|-------|----------------|
| ND 4-bands: (b2-b1)/(b3+b4) | 560, 2190, 1610, 1610 | 0.69 | 16.01 | 0.79 |
| ND 3-bands: (b2-b1)/(b2+b3) | 560, 2190, 740 | 0.70 | 16.74 | 0.79 |
| ND 2-bands: (b2-b1)/(b2+b1) | 665, 560 | 0.76 | 16.86 | 0.74 |
| SR 2-bands: (b2/b1) | 665, 560 | 0.77 | 20.36 | 0.74 |

A 4-band SI with bands in green and SWIR best validated. Green and red led to best 2-band index.

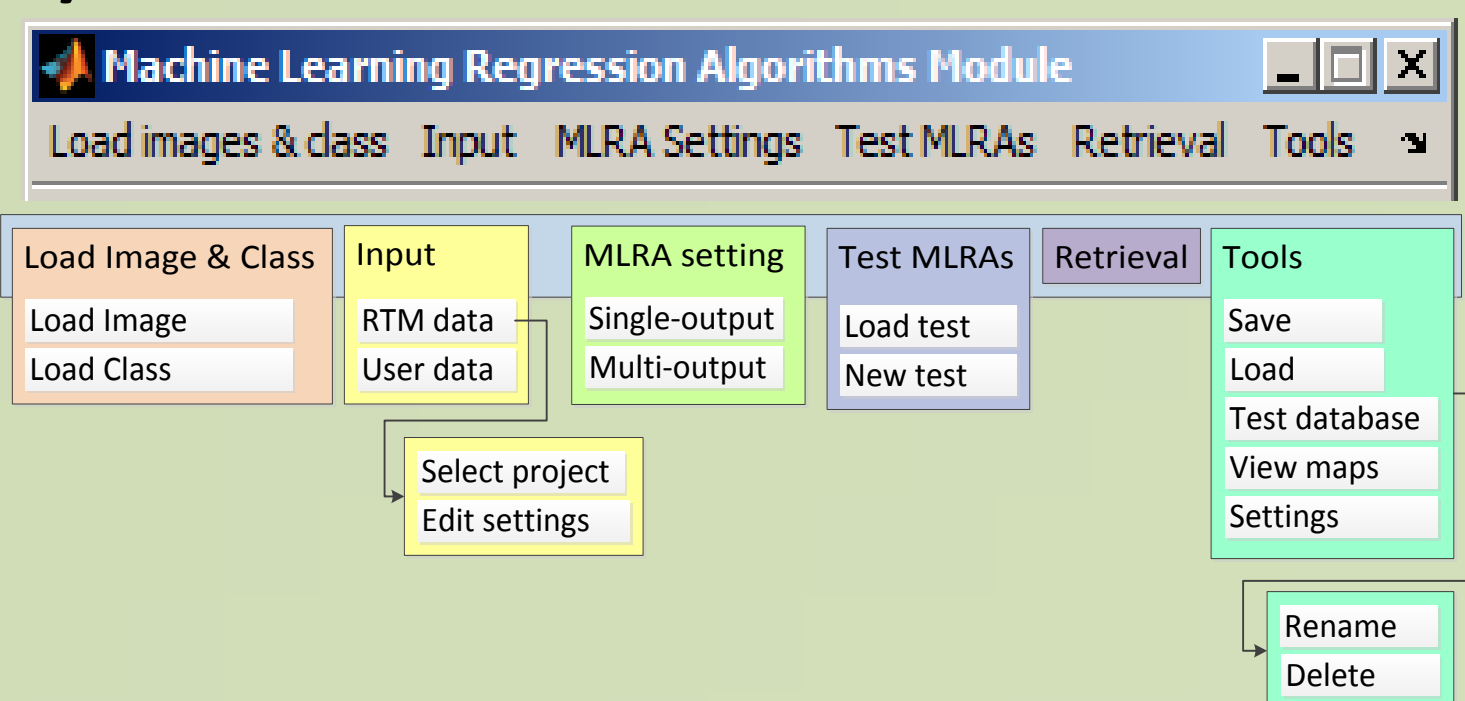


Map (1 layer) generated in 1.1 s.



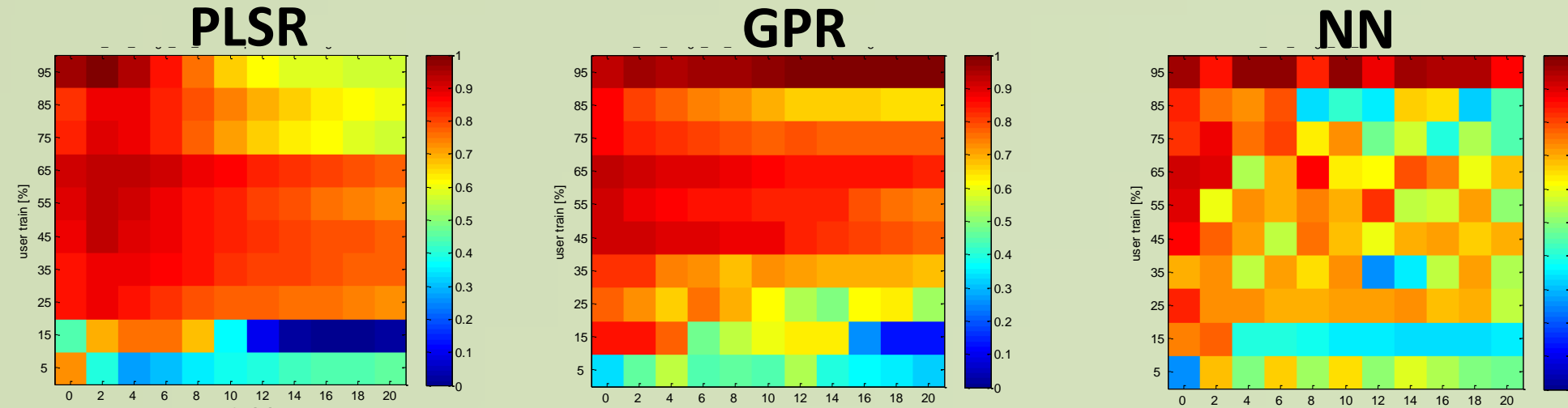
4. (ii) Nonparametric regression: Machine learning regression algorithms (MLRAs) - LAI

ARTMO's Machine Learning Regression Algorithms (MLRA) module:



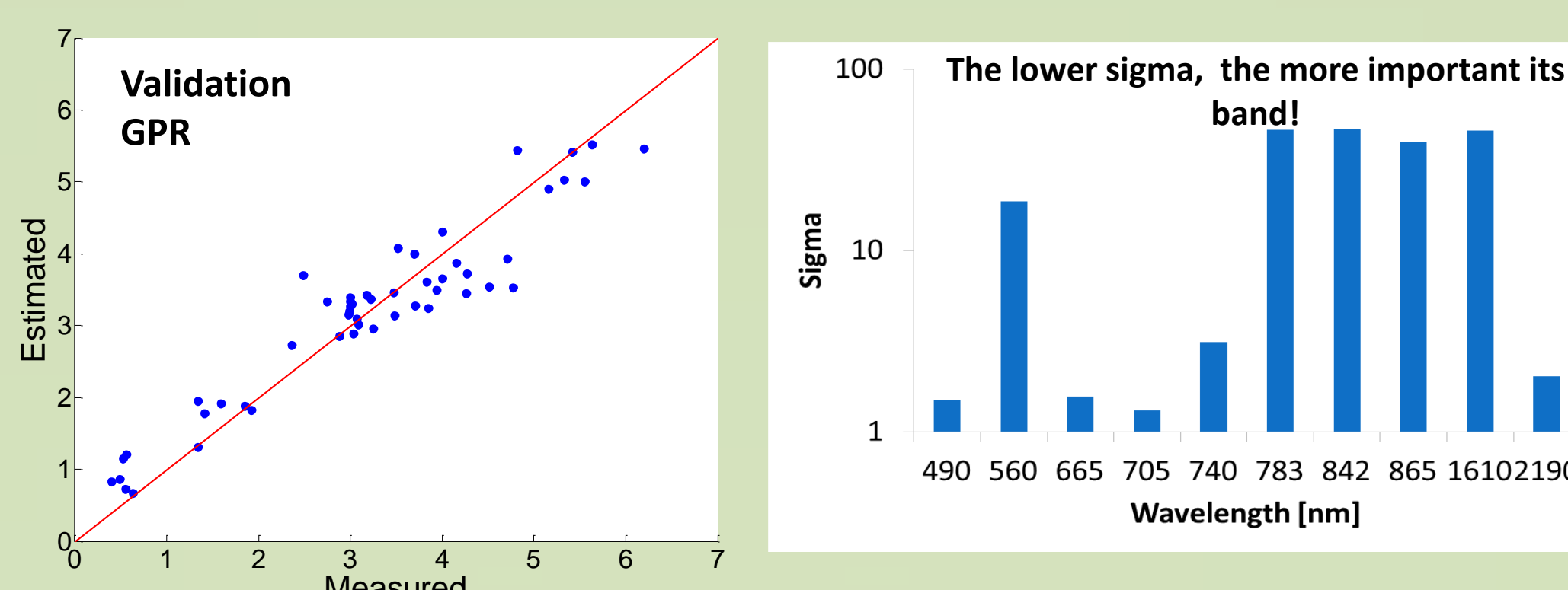
- **More than 10 MLRAs** have been implemented, e.g. neural nets (NN), kernel ridge regression (KRR), Gaussian Processes regression (GPR), principal component regression (PCR), partial least squares regression (PLSR), regression trees (RT) - (<http://www.uv.es/gcamps/code/simpleR.html>).
- Options to add noise and partitionate training-validation are provided.

Examples of **robustness**: validation results (R²) along increasing noise levels (X) and training data (Y):

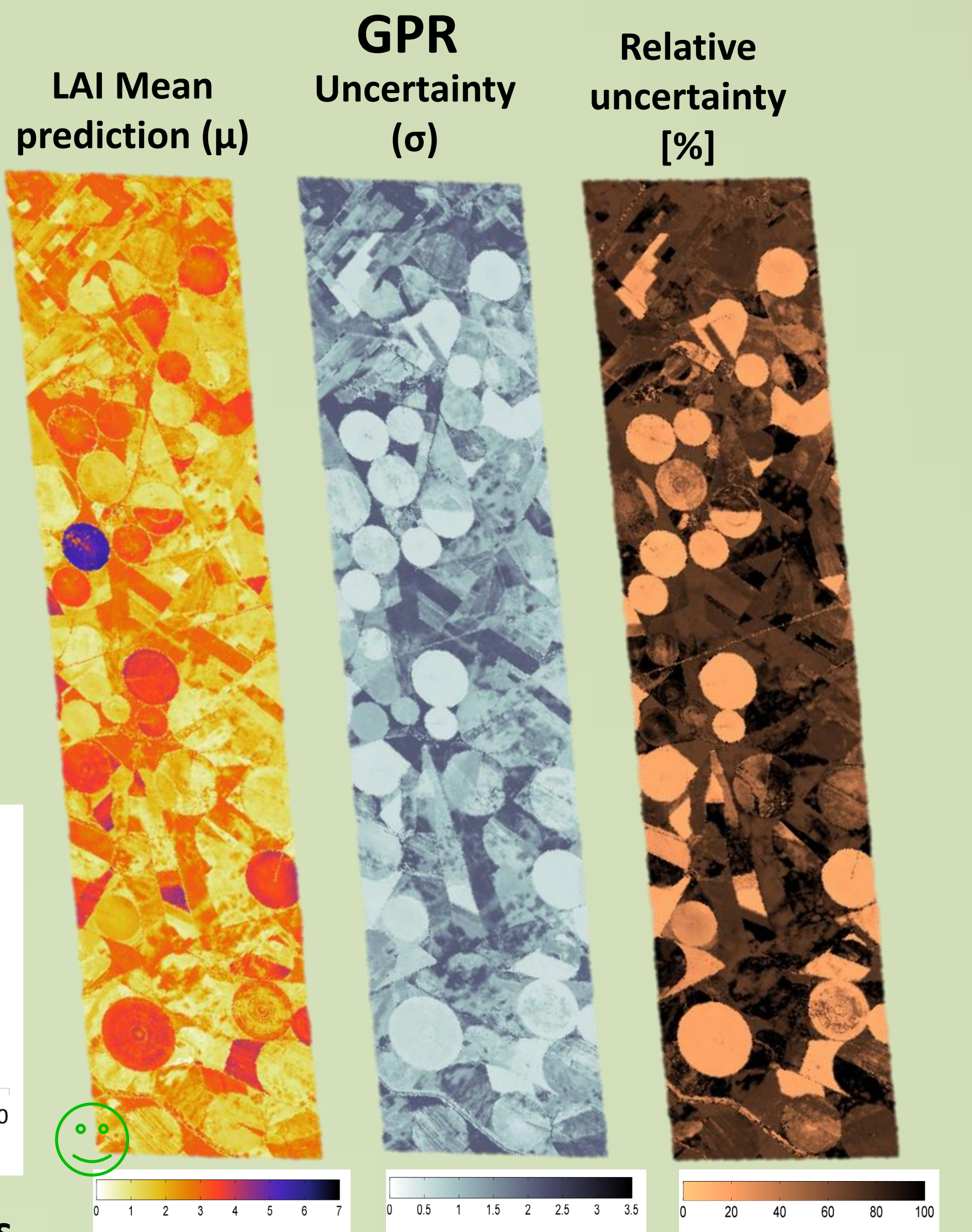


50% validation results ranked according to R²:

| MLRA | RMSE | NRMSE | R ² | Time (s.) |
|--------------------------------------|-------------|-------------|----------------|-----------|
| Kernel ridge Regression | 0.41 | 7.04 | 0.93 | 0.063 |
| Gaussian Processes Regression | 0.47 | 8.17 | 0.91 | 0.788 |
| Neural Network | 0.46 | 7.99 | 0.91 | 6.069 |
| VH. Gaussians Processes Regression | 0.48 | 8.30 | 0.90 | 2.473 |
| Extreme Learning Machine | 0.48 | 8.26 | 0.89 | 0.061 |
| Bagging trees | 0.58 | 10.03 | 0.87 | 1.296 |
| Relevance vector Machine | 0.59 | 10.20 | 0.86 | 16.501 |
| Least squares linear regression | 0.56 | 9.62 | 0.86 | 0.002 |
| Boosting trees | 0.70 | 12.10 | 0.79 | 1.100 |
| Partial least squares regression | 0.71 | 12.16 | 0.78 | 0.008 |
| Regression tree | 0.78 | 13.46 | 0.72 | 0.006 |
| Principal components regression | 0.79 | 13.70 | 0.71 | 0.002 |

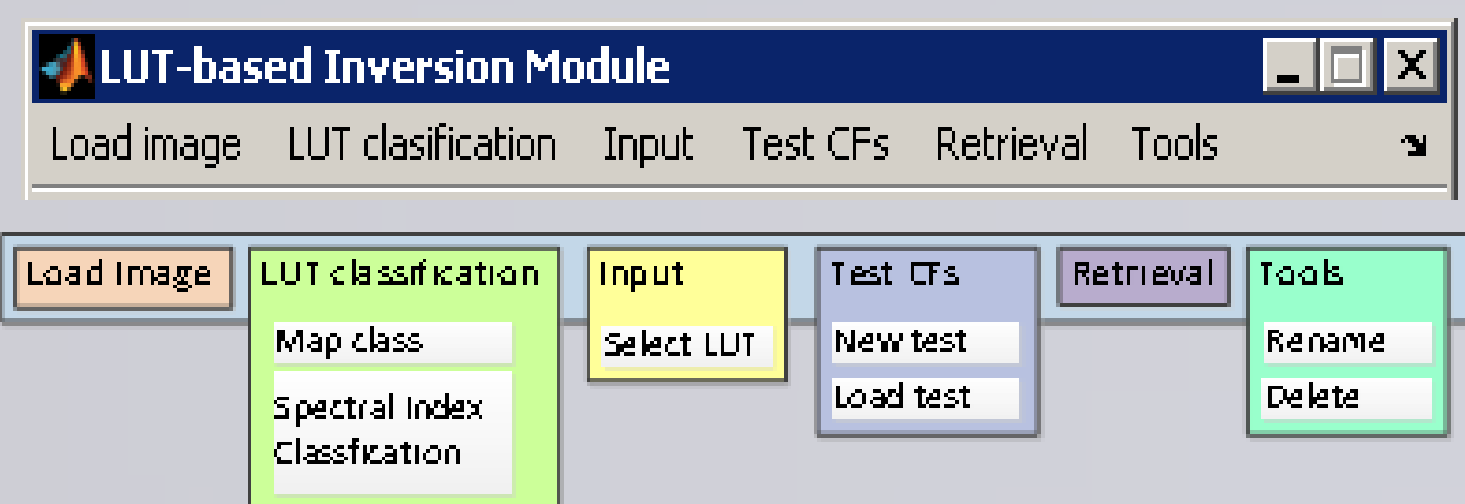


Map (3 layers) generated in 7.5 s.



5. (iii) Inversion of canopy RTM through cost functions - LAI

ARTMO's Inversion module:



- Retrieval of biophysical parameters through LUT-based inversion.
- LUTs prepared in ARTMO and loaded in **Inversion** module
- **More than 60 cost functions** have been implemented.
- Various regularization options: adding noise, mean of multiple solutions, data normalization.

PROSAIL LUT (sub-selection 100000):

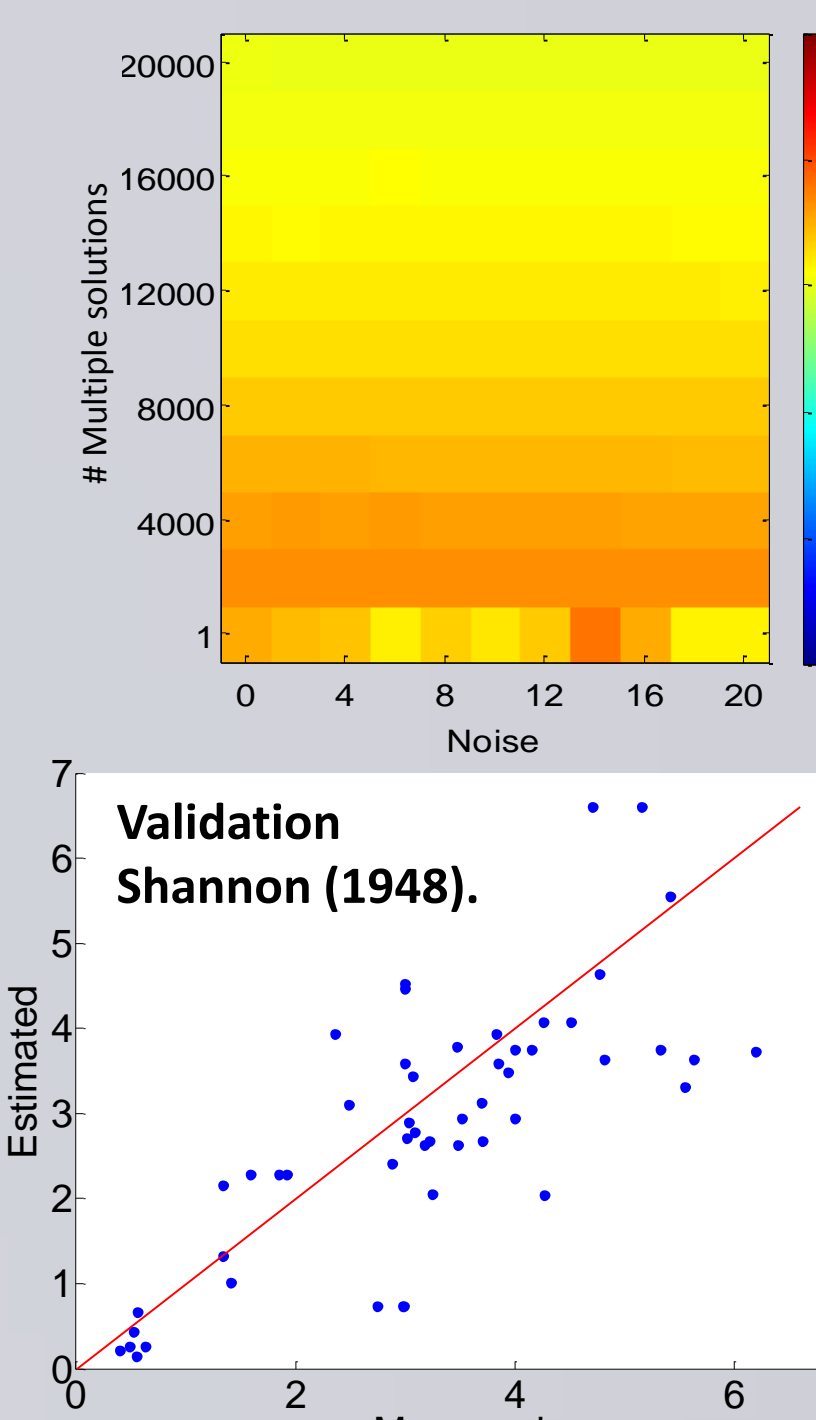
| Model Parameters | Units | Range | Distribution |
|-----------------------------------|----------------------------------|-----------------------------------|--------------------------|
| Leaf variables: PROSPECT-4 | | | |
| N | Leaf structure index | unitless | 1.1 |
| ALA | Leaf chlorophyll content | (µg/cm ²) | 5-75 |
| LCC | Leaf chlorophyll content | (µg/cm ²) | Gaussian (x: 35, SD: 30) |
| C _m | Leaf dry matter content | (g/cm ²) | 0.001-0.03 |
| C _w | Leaf water content | (cm) | 0.002-0.05 |
| Canopy variables: 4SAIL | | | |
| LAI | Leaf area index | (m ² /m ²) | 0.1-7 |
| ω _{soil} | Soil scaling factor | unitless | 0 |
| ALA | Average leaf angle | (°) | 40-70 |
| HotS | Hot spot parameter | (m/m) | 0.05-0.5 |
| skyl | Diffuse incoming solar radiation | (fraction) | 0.05 |
| θ ₁ | Sun zenith angle | (°) | 22.3 |
| θ _v | View zenith angle | (°) | 0 |
| φ | Sun-sensor azimuth angle | (°) | 0 |

Examples of cost functions:
Shannon (1948):
 $D(P, Q) = - \sum_{\lambda_i} \frac{p(\lambda_i) + q(\lambda_i)}{2} \log \left(\frac{p(\lambda_i) + q(\lambda_i)}{2} \right) + \frac{1}{2} \left(\sum_{\lambda_i} p(\lambda_i) \log(p(\lambda_i)) + \sum_{\lambda_i} q(\lambda_i) \log(q(\lambda_i)) \right)$
Laplace distribution:
 $D(P, Q) = \sum_{\lambda_i=1}^n |p(\lambda_i) - q(\lambda_i)|$
Pearson chi-square:
 $D(P, Q) = \sum_{\lambda_i=1}^n \frac{(q(\lambda_i) - p(\lambda_i))^2}{p(\lambda_i)}$

In total 5508 inversion strategies analyzed. **50% validation results** for best noise & multiple samples ranked according to R²:

| Cost function | % Noise | % multiple samples | RMSE | NRMSE | R ² | time (s.) |
|-----------------------|-----------|--------------------|-------------|--------------|----------------|-----------|
| Shannon (1948) | 14 | single best | 0.96 | 16.56 | 0.76 | 0.027 |
| Laplace distribution | 6 | single best | 0.86 | 14.74 | 0.74 | 0.021 |
| Neyman chi-square | 0 | single best | 0.89 | 15.31 | 0.74 | 0.005 |
| Pearson chi-square | 16 | single best | 1.03 | 17.74 | 0.73 | 0.005 |
| Least absolute error | 6 | single best | 0.89 | 15.28 | 0.72 | 0.005 |
| Geman and McClure | 16 | 2 | 0.83 | 14.36 | 0.71 | 0.007 |
| RMSE | 16 | 2 | 0.83 | 14.37 | 0.71 | 0.006 |
| Exponential | 16 | 2 | 0.85 | 14.66 | 0.71 | 0.008 |
| K(x)=x(log(x))-x | 20 | single best | 1.06 | 18.25 | 0.70 | 0.009 |
| K(x)=(log(x))^2 | 0 | 2 | 1.01 | 17.40 | 0.69 | 0.012 |
| K-divergence Lin | 4 | single best | 2.60 | 44.84 | 0.64 | 0.009 |
| Shannon entropy | 6 | 2 | 1.15 | 19.82 | 0.60 | 0.013 |
| Gen. Kullback-Leibler | 10 | 2 | 1.20 | 20.63 | 0.58 | 0.013 |
| Neg. Exp. disparity | 0 | 4 | 1.04 | 17.96 | 0.58 | 0.007 |
| Kullback-leibler | 4 | 18 | 1.66 | 28.62 | 0.57 | 0.009 |
| K(x)=log(x)+1/x | 2 | single best | 2.07 | 35.65 | 0.55 | 0.012 |
| Harmonique Toussaint | 2 | 20 | 1.57 | 27.04 | 0.54 | 0.005 |
| K(x)=-log(x)+x | 2 | 2 | 1.77 | 30.52 | 0.49 | 0.012 |

Example of **robustness** (R²) along increasing noise levels (X) and mean of multiple solutions (Y) in the Shannon (1948) Cost Function inversion:



Map (4 layers) generated in 90925.9 s. (> 25 hours)

